

## Lack of optical activity in the incommensurate phases of $\text{Rb}_2\text{ZnBr}_4$ and $[\text{N}(\text{CH}_3)_4]_2\text{CuCl}_4$

J. Ortega, J. Etxebarria, J. Zubillaga, T. Brezewski,\* and M. J. Tello

*Departamento de Física de la Materia Condensada, Facultad de Ciencias, Universidad del País Vasco, Apartado 677, 48080 Bilbao, Spain*

(Received 24 May 1991)

The optical activity of  $\text{Rb}_2\text{ZnBr}_4$  and  $[\text{N}(\text{CH}_3)_4]_2\text{CuCl}_4$  has been measured in their centrosymmetric incommensurate phases using a high-accuracy universal polarimeter (HAUP). The results obtained show a zero value of this quantity along all the measured directions (two in the case of  $\text{Rb}_2\text{ZnBr}_4$  and one for the  $[\text{N}(\text{CH}_3)_4]_2\text{CuCl}_4$  crystal). This behavior differs from results published previously for these or other similar incommensurate materials. The present measurements are compared with those reported in these previous studies, analyzing, in view of the differences, the possible sources of systematic errors in the HAUP technique. Our experimental results are in accordance with the idea that gyration tensors in incommensurate structures must be symmetry restricted, in a conventional manner, by the point group associated to their superspace group. Recent models allowing the appearance of gyration effects in incommensurate crystals with inversion symmetry should be reconsidered in the light of our results.

### I. INTRODUCTION

The so-called high-accuracy universal polarimeter (HAUP) permits one to measure the optical activity (OA) in birefringent crystal sections. Since the development of this technique by Kobayashi and Uesu in 1983,<sup>1</sup> the gyration tensor has been studied for a small number of materials. In particular, the presence of gyration effects has been detected in some directions of the incommensurate (INC) phases of the following materials:  $\text{K}_2\text{SeO}_4$ ,  $(\text{NH}_4)_2\text{BeF}_4$ ,  $[\text{N}(\text{CH}_3)_4]_2\text{ZnCl}_4$ ,  $[\text{N}(\text{CH}_3)_4]_2\text{CuCl}_4$ ,  $\text{Rb}_2\text{ZnCl}_4$ , and  $\text{Rb}_2\text{ZnBr}_4$ .<sup>2-10</sup> The theoretical interpretation of this effect is difficult because all these phases are centrosymmetric, and in principle, no optical activity should be allowed. Furthermore, a rotation of the optical indicatrix, also symmetry forbidden, has been observed in the INC phases of  $[\text{N}(\text{CH}_3)_4]_2\text{CuCl}_4$ ,<sup>2</sup>  $\text{MnBaF}_4$ ,<sup>11</sup> and  $(\text{CH}_3)_3\text{NCH}_2\text{COO} \cdot \text{CaCl}_2 \cdot 2\text{H}_2\text{O}(\text{BCCD})$ .<sup>12</sup>

From the experimental point of view, the measurement of these effects is problematic even with the HAUP device. This is so because the birefringence is typically 1000 times larger than the gyration coefficients. In fact, in the only INC material studied by more than one group ( $[\text{N}(\text{CH}_3)_4]_2\text{ZnCl}_4$ ), up to three different values for the gyration coefficient  $g_{13}$  (setting  $Pcmn$ ) have been reported. Namely, different temperature behaviors are found in Refs. 2 and 5, and although the results of Refs. 5 and 9 have a qualitatively similar temperature dependence, the data differ by about one order of magnitude.

In view of this situation it seems of interest to provide more experimental information about the OA in INC centrosymmetric crystals as well as to study more thoroughly the sources of errors in the experimental procedures. In this paper we report on detailed studies of the OA and birefringence on two materials:  $\text{Rb}_2\text{ZnBr}_4$  and  $[\text{N}(\text{CH}_3)_4]_2\text{CuCl}_4$ . The measurements have been performed in the normal and INC phases of both crystals us-

ing a HAUP system built up in our laboratory. The results show a zero value of the OA along all the measured directions. This is in accordance with the idea that the gyration tensors in INC structures are restricted by the point groups associated to their superspace groups. However, as this behavior is in great contrast to that found in the works referred to above, it has been considered important to present a detailed description of the experimental procedure, data collection, and refinement. This is done in Sec. II, where special attention is paid to showing some sources of systematic errors which can appear when working with the HAUP technique. Likewise, in order to provide a basic validation of the results obtained with our HAUP equipment, we present measurements of the OA and birefringence of  $\alpha$ -quartz along the direction perpendicular to the optical axis. The OA results in the INC materials are shown in Sec. III. In Sec. IV some possible errors in the experimental procedure are analyzed and the OA results are compared with other published measurements. Finally, the results are discussed in the light of the available theories for INC structures.

### II. EXPERIMENTAL PROCEDURE

#### A. Description of the experimental setup

Figure 1 shows a block diagram of our HAUP apparatus. The light of a 10-mW He-Ne laser passes a polarizer, the sample, and an analyzer. Before entering the photomultiplier, the light goes through an interference filter (with a bandwidth of 0.8 nm) and several diaphragms which block the scattered light. The polarizers are Glan-Thompson prisms of the highest commercial grade mounted on two rotating stages driven by continuous motors. The resolution of the motors is approximately  $\pm 2.7 \times 10^{-6}$  rad. An encoder motor controller guarantees the reproducibility of the angular positions

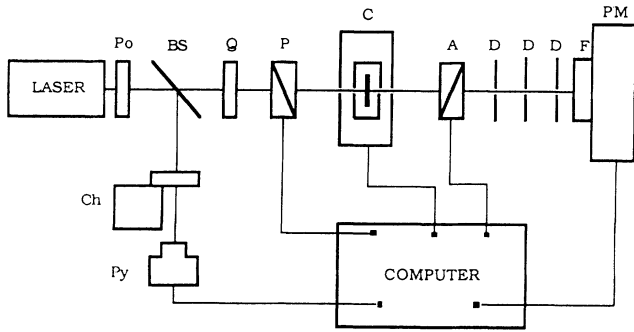


FIG. 1. Schematic diagram of the HAUP equipment. Po, Polaroid film; BS, beam splitter; Q, quarter-wave plate; P, polarizer; C, sample cryostat; A, analyzer; D, diaphragm; F, interference filter; PM, photomultiplier; Ch, mechanical chopper; Py, pyroelectric detector.

within  $\pm 8.1 \times 10^{-6}$  rad for each motor movement. The sample is installed into a furnace which allows for a temperature stability of  $0.1^\circ\text{C}$  between room temperature and  $300^\circ\text{C}$ . The pyroelectric detector is used to compensate the intensity fluctuations of the laser, and after the beam splitter, a quarter-wave plate is placed in the main branch of the apparatus, in such a way that the light before the polarizer is circular. This ensures that no variations of the light intensity will occur after the light passage through the first polarizer. The temperature of the laboratory is kept constant within  $1^\circ\text{C}$ . If no temperature control is used, a clear variation of the transmitted intensity is found. The origin of this effect could be a drift in the photomultiplier output or electronics or, perhaps, a change in the ellipticity of the polarizers, as suggested by Moxon.<sup>13</sup>

No optical components are placed between the sample and polarizers, and even the windows of the furnace are removed. This is very important because the residual strain birefringence of the windows can produce systematic errors which make the final results completely unreliable. This point will be explained more thoroughly in Sec. IV.

### B. Data collection and analysis

The measurement process is as follows. Before setting the sample in place, an accurate determination is made of the crossed-polarizer position. After inserting the crystal and for each temperature, the transmitted intensity is measured as a function of the polarizer position  $\Theta$  and relative polarizer-analyzer angle  $Y$ . For a fixed  $\Theta$  value, 11  $Y$  values are scanned in steps of  $1.6 \times 10^{-3}$  rad around the region where the intensity is minimum. The process is repeated for a total of 11  $\Theta$  positions. The polarizer angles are also varied in steps of  $1.6 \times 10^{-3}$  rad in such a way that the resulting  $(Y, \Theta)$  region is centered around the absolute minimum of the transmitted intensity.

The data are analyzed in terms of the equation<sup>1,14</sup>

$$\Gamma = A + B\Theta + C(Y\Theta + \Theta^2) + DY + Y^2, \quad (1)$$

with

$$A = A_0 + (p + q)^2 + 4 \sin^2 \Delta / 2 [k^2 - k(p + q) - pq],$$

$$B = 2(p + q) \sin \Delta,$$

$$C = 4 \sin^2 \Theta / 2,$$

$$D = -2(k - p) \sin \Delta.$$

In Eq. (1),  $\Gamma$  is the transmitted intensity relative to that of the incoming light,  $A_0$  a constant accounting for the stray light,  $p$  and  $q$  the (intrinsic) parasitic ellipticities of the polarizers,  $\Delta$  the phase difference of the sample, which can be approximated by  $2\pi/\lambda \Delta n d$ , and  $k = G/(2\bar{n} \Delta n)$ .  $G$ ,  $\Delta n$ , and  $\bar{n}$  are the optical activity, birefringence, and mean refractive index, respectively, of the sample,  $d$  its thickness, and  $\lambda$  the light wavelength in vacuum.

Instead of fitting the results according to the process used by Kobayashi and Uesu<sup>1</sup> (i.e., a fit in  $Y$  and a further fit of the obtained parameters in  $\Theta$ ), we employ a linear least-squares fit of all the experimental data in terms of five basis functions

$$1, \Theta, Y\Theta + \Theta^2, Y, Y^2.$$

This procedure, suggested in Ref. 14 and used in Ref. 15, improves the quality of the final parameters since it permits us to organize easily a weighting scheme for the fit and provides a unique goodness-of-fit value per point. Once  $A$ ,  $B$ ,  $C$ , and  $D$  are calculated, the following coefficients are obtained:

$$\Theta_0 = -B/2C = -(p + q)/2 \cot \Delta / 2,$$

$$C' = C = 4 \sin^2 \Delta / 2, \quad (2)$$

$$D' = D - B/2 = -(2k - \gamma) \sin \Delta,$$

where  $\gamma = p - q$ .  $\Theta_0$  can be interpreted as the polarizer position that corresponds to a minimum light intensity between crossed polarizers. Evidently, as  $\Theta$  is referred to an arbitrary origin, only the relative variations of  $\Theta_0$  are experimentally accessible.

Up to now we have assumed that the angle  $Y$  could be determined with an arbitrary degree of accuracy. Nevertheless, Kobayashi, Kumoni, and Saito<sup>5</sup> found that, because of sample misalignment or imperfections in the polarizers, there was an apparent error  $\delta Y$  that should be considered. However, as pointed out by Moxon and Renshaw,<sup>14</sup> none of these reasons can introduce in practice a  $\delta Y$  value of the observed magnitude. The appearance of this error is presumably connected with the roughness of the sample surface<sup>13</sup> or mechanical drifts of the motor drivers during the course of the experiment. In our apparatus drifts of the order of  $2 \times 10^{-4}$  rad have been observed from the initial crossed-polarizer position after the time of a typical experiment. This is the order of magnitude found for  $\delta Y$  in all cases when samples polished to a local flatness of  $1 \mu\text{m}$  are used.

With the  $\delta Y$  error included, Eqs. (2) take the form<sup>5</sup>

$$\Theta_0 = -(p + q)/2 \cot \Delta / 2 - \delta Y / 2,$$

$$C' = C = 4 \sin^2 \Delta / 2, \quad (3)$$

$$D' = D - B/2 = -(2k - \gamma) \sin \Delta + 2 \delta Y \cos^2 \Delta / 2.$$

The birefringence is finally obtained from  $C'$  with a previous knowledge of the sign of  $\partial\Delta/\partial T$  and the absolute value of  $\Delta$  at one temperature  $T$ . The OA is obtained from  $D'/\sin\Delta$  once the data are corrected from the  $\gamma$  and  $\delta Y$  errors. In the measurements presented in Sec. III, these parameters have been calculated from a linear fit<sup>5</sup> of  $D'/\sin\Delta$  vs  $\cot \Delta/2$  in the parent phase of  $[\text{N}(\text{CH}_3)_4]_2\text{CuCl}_4$  and  $\text{Rb}_2\text{ZnBr}_4$ , where, according to symmetry requirements, the OA should be zero.

If the material under study presents OA in all the temperature range studied,  $\gamma$  and  $\delta Y$  must be obtained from a second measurement with the crystal rotated by  $90^\circ$  (Ref. 14) or using a check crystal with  $G=0$ .<sup>16</sup> This is the case for  $\alpha$ -quartz, which was used as a standard in order to check our HAUP setup and the measuring method. In this case measurements were performed along the direction perpendicular to the optic axis on a 0.180-mm-thick platelet. The temperature was scanned between 22 and  $100^\circ\text{C}$ , and the error constants were calculated by adopting the method proposed in Ref. 14. The  $\Delta n$  results were found to be in very good agreement with the published values.<sup>16</sup> Regarding the OA, an almost constant  $2k$  was obtained in the whole temperature range,  $2k = -3.96 \times 10^{-3}$ . Since the OA of quartz is known to have different signs along and perpendicular to the optic axis, the negative value of  $2k$  means that our quartz sample is dextrorotatory for light propagating along the optic axis. The values scattered within a range of  $\pm 3.5 \times 10^{-5}$ , which is rather accurate for this kind of measurements. These results are in agreement with those published at room temperature in Ref. 15. In contrast, the  $2k$  values obtained in Ref. 16 for dextrorotatory quartz (in which the check-crystal method was employed) are somewhat different. This is strange, however, because our  $2k$  is (except the sign) consistent with the  $g_{11}$  value reported in the same work for the laevorotatory specimen.

### III. EXPERIMENTAL RESULTS

#### A. $\text{Rb}_2\text{ZnBr}_4$

$\text{Rb}_2\text{ZnBr}_4$  undergoes a phase transition from the paraelectric  $Pcmm$  phase to an INC phase at  $T_i = 76^\circ\text{C}$ . The INC phase can be described by the superspace group  $Pcmm(00\gamma)(ss-1)$ , the modulation wave vector being  $\mathbf{q} = \gamma\mathbf{c}^*$  ( $\gamma \approx 1/3$ ).<sup>17</sup> At  $T_c = -83^\circ\text{C}$  the modulation becomes commensurate,  $\mathbf{q} = 1/3\mathbf{c}^*$ , and a ferroelectric lock-in phase appears, with space group  $Pc2_1n$ . At room temperature the cell parameters of the basic structure are  $a = 13.33 \text{ \AA}$ ,  $b = 7.66 \text{ \AA}$ , and  $c = 9.71 \text{ \AA}$ .

Single crystals of  $\text{Rb}_2\text{ZnBr}_4$  were grown from an aqueous solution using a dynamic method.<sup>18</sup> Large colorless crystals exhibiting clear natural faces were obtained. Two samples cut in the directions of the (011) and (101) planes were used for the measurements. The thicknesses were 0.706 and 0.747 mm, respectively.

The results obtained for  $C'$  and the derived birefringence are given in Figs. 2 and 3. In order to obtain the absolute birefringence, the  $C'$  data were supplemented with a measurement at  $22^\circ\text{C}$  of the optical retar-

ation by using a Berek compensator. The INC transition is clearly visible at  $76^\circ\text{C}$ . Above  $T_i$  the slope of  $\Delta n$  increases for the (011) sample and decreases for the (101) sample. The results are consistent with those reported by Meekes and Janner.<sup>8</sup>

Figures 4 and 5 show the temperature dependence of  $D'/\sin\Delta$  for both samples, and the derived curves of  $2k$  are plotted in Figs. 6 and 7. Solid circles were obtained by fitting  $D'/\sin\Delta$  to  $\cot \Delta/2$  only in the normal phase, whereas open symbols resulted under the assumption of a zero  $G$  value in both phases. The  $\gamma$  and  $\delta Y$  parameters were determined to be  $\gamma = -2.6$  and  $-2.7 \times 10^{-3}$ ,  $\delta Y = -2.1$  and  $-2.0 \times 10^{-3}$  for the (011) sample and  $\gamma = -3.9$  and  $-1.4 \times 10^{-5}$ ,  $\delta Y = 7.1$  and  $3.1 \times 10^{-5}$  for the (101) sample. The difference of two orders of magnitude in the corresponding error constants for both samples can be attributed to their different quality (the first was clearly worse because it was not polished down to  $1 \mu\text{m}$  and had small defects on its surface). Also, the drift of the motor drivers during the measurement of the second sample was found to be smaller than usual ( $\approx 10^{-5}$  rad). Anyway, the conclusion is the same with both samples: There is no measurable OA in the INC phase. A conservative upper bound for the  $2k$  value can be  $7 \times 10^{-5}$  for the (011) sample and  $5 \times 10^{-5}$  for the (101) case. It is worth noting the accuracy obtained for  $2k$ , which presents a noise one or two orders of magni-

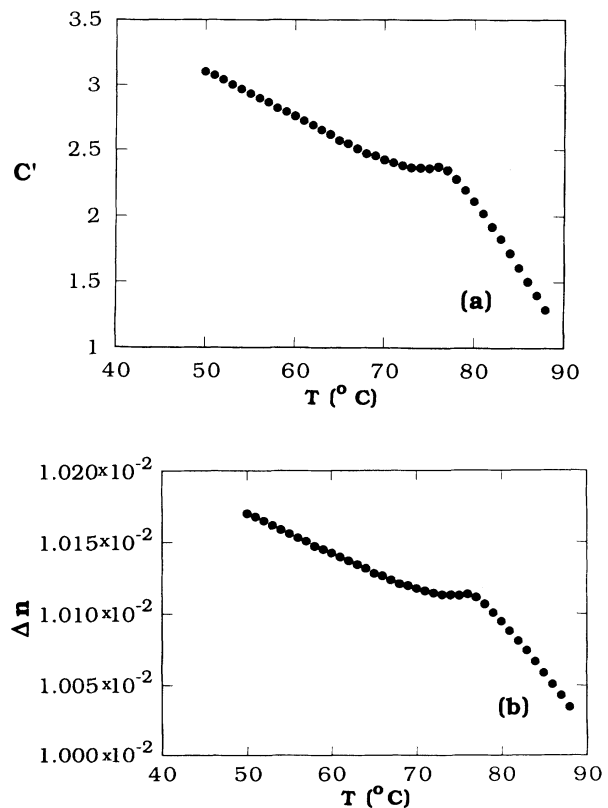


FIG. 2. (a) Temperature dependence of  $C' = 4 \sin^2 \Delta / 2$  for the (011) sample of  $\text{Rb}_2\text{ZnBr}_4$ . (b) Birefringence data obtained from (a).

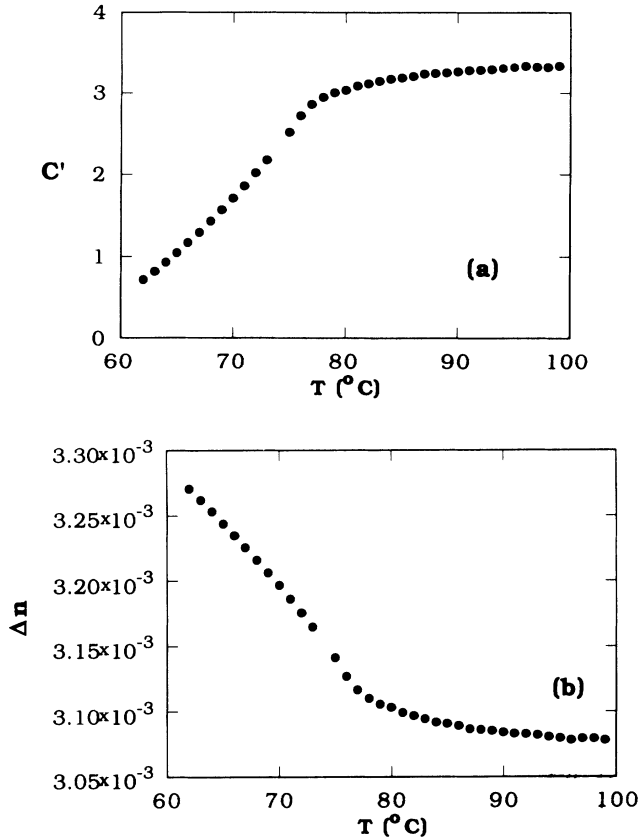


FIG. 3. (a) Temperature dependence of  $C' = 4 \sin^2 \Delta / 2$  for the (101) sample of  $\text{Rb}_2\text{ZnBr}_4$ . (b) Birefringence data obtained from (a).

tude smaller than what is considered usual in these measurements.

The OA measured is related to the  $g_{ij}$  coefficients by the expression

$$G = \sum g_{ij} n_i n_j \quad (4)$$

where  $\mathbf{n}$  is the unit vector in the direction of the incident light. Equation (4) together with the above results implies that, unless an accidental compensation takes place

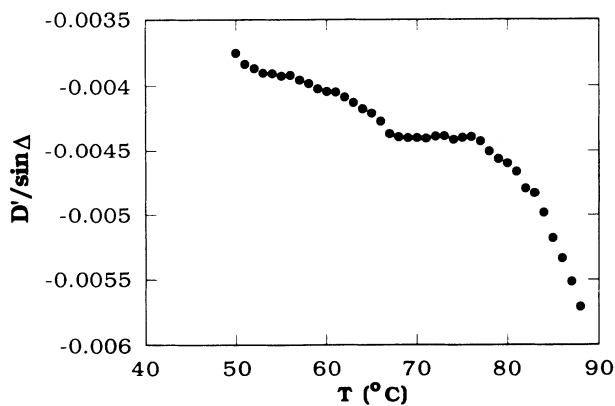


FIG. 4. Temperature dependence of  $D'/\sin\Delta = -(2k - \gamma) + \delta Y \cot\Delta/2$  for the (011) sample of  $\text{Rb}_2\text{ZnBr}_4$ .

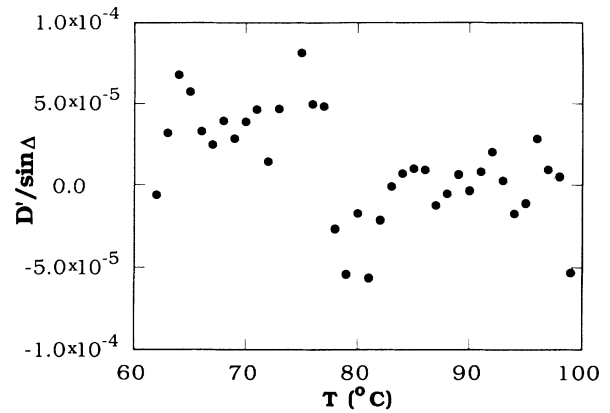


FIG. 5. Temperature dependence of  $D'/\sin\Delta = -(2k - \gamma) + \delta Y \cot\Delta/2$  for the (101) sample of  $\text{Rb}_2\text{ZnBr}_4$ .

in the INC range, all the  $g_{ij}$  (except  $g_{12}$ ) are zero in this phase.

### B. $[\text{N}(\text{CH}_3)_4]_2\text{CuCl}_4$

$[\text{N}(\text{CH}_3)_4]_2\text{CuCl}_4$  (TMACuCl) exhibits an INC phase between  $T_i = 26^\circ\text{C}$  and  $T_c = 20^\circ\text{C}$ . The space groups of the parent and lock-in phases are  $Pcmn$  and  $P2_1/c11$ , respectively.<sup>19</sup> At room temperature the cell parameters are  $a = 15.59 \text{ \AA}$ ,  $b = 9.03 \text{ \AA}$ , and  $c = 12.30 \text{ \AA}$ . The modulation of the INC phase is along the  $c^*$  axis, with a wave vector  $\mathbf{q} = \gamma \mathbf{c}^*$  ( $\gamma \approx \frac{1}{3}$ ). The only superspace group that can give rise to the observed phase sequence is  $Pcmn(00\gamma)(ss-1)$ .<sup>20</sup>

Single crystals of TMACuCl were grown by very slow evaporation of an aqueous solution containing stoichiometric amounts of  $[\text{N}(\text{CH}_3)_4]\text{Cl}$  and  $\text{CuCl}_2$ . The crystals obtained had platelike shape with the main faces perpendicular to the (pseudo)hexagonal  $c$  axis. One of these platelets, 0.435 mm thick, polished with 1- $\mu\text{m}$  grain-size diamond paste, was the sample used in our experiments.

Figure 8(a) shows the temperature dependence of the

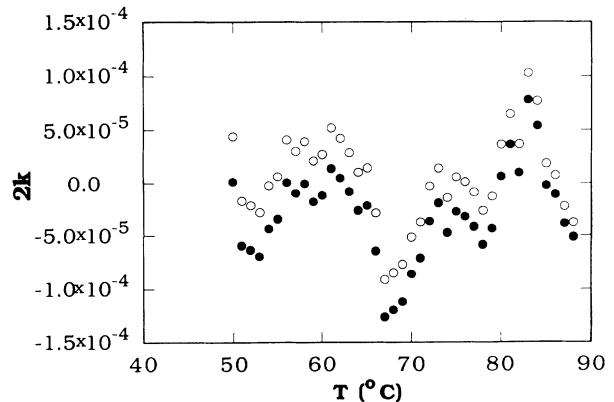


FIG. 6.  $2k$  values for the (011) sample of  $\text{Rb}_2\text{ZnBr}_4$ . The data were deduced assuming a zero OA in the paraelectric phase (solid circles) or in all the temperature range (open circles).

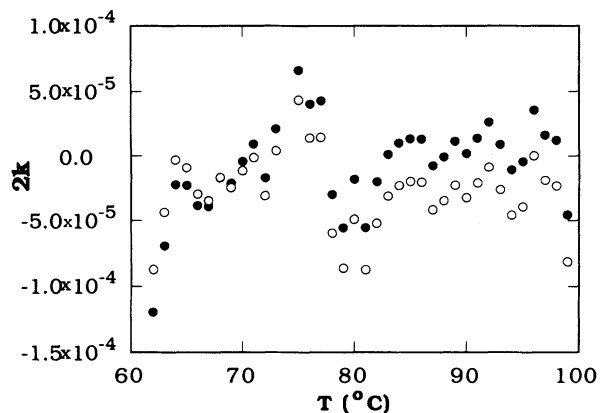


FIG. 7. Temperature dependence of  $2k$  for the (101) sample of  $\text{Rb}_2\text{ZnBr}_4$ . The data were deduced assuming a zero OA in the paraelectric phase (solid circles) or in all the temperature range (open circles).

quantity  $C'$ , and the derived birefringence curve is plotted in Fig. 8(b). In the same way as for  $\text{Rb}_2\text{ZnBr}_4$ , the absolute  $\Delta n$  was deduced from an independent measurement of the optical retardation at  $22^\circ\text{C}$  using a compensator. The INC phase transition is clearly visible at

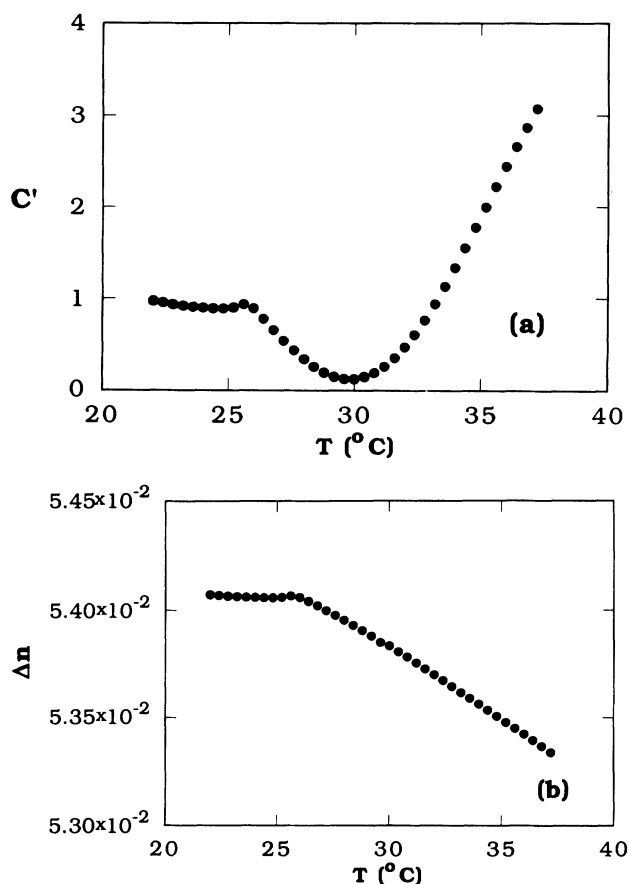


FIG. 8. (a) Temperature dependence of the quantity  $C' = 4 \sin^2 \Delta / 2$  for  $\text{TMAcCl}$  along the  $c$  axis. (b) Birefringence deduced from  $C'$ . The INC transition at  $T_i = 26^\circ\text{C}$  is clearly visible.

$T = 26^\circ\text{C}$ . As can be seen,  $\Delta n$  presents a clear change of slope at the transition. A similar behavior has been found before for the relative  $\Delta n$  change,<sup>21,22</sup> although the absolute values of  $\Delta n$  reported by Gómez-Cuevas *et al.*<sup>21</sup> differ from ours by two orders of magnitude. This discrepancy was due to a mistake in the identification of the Newton color sequence in this highly colored material. This point has also been noted by Saito, Sugiya, and Kobayashi,<sup>7</sup> who have reported an absolute  $\Delta n$  value of the same order of ours for the direction along the bisector between the  $b$  and  $c$  axes.

Figure 9 shows the temperature behavior of the quantity  $D'/\sin\Delta$ . A marked contangentlike singularity appears around  $T = 30^\circ\text{C}$ , which occurs when  $C'$  is close to zero. However, in contrast with the  $\Delta n$  data, only a very small effect whose size does not allow for a clear separation from the experimental noise is observed at the transition. This can be appreciated better in Fig. 10, where the OA data corrected from the  $\gamma$  and  $\delta Y$  errors are plotted as a function of temperature. The meaning of the solid and open symbols in these figures is the same as in Fig. 6. The parameters  $\gamma$  and  $\delta Y$  were determined to be  $\gamma = -3.1$  and  $-3.4 \times 10^{-4}$ ,  $\delta Y = 4.3$  and  $4.3 \times 10^{-4}$  in both fits. As can be seen, data near  $30^\circ\text{C}$  are of worse quality than the rest because the singularity is not fully suppressed. Noise is smaller at the INC range, which is out of the region of the singularity. However, even there, the presence of any OA cannot be assured because of the proximity of the singularity to the INC phase, the experimental error of  $D'$ , and the uncertainty of the constants  $\gamma$  and  $\delta Y$ . As can be seen, assuming a zero  $G$  value only above  $26^\circ\text{C}$  leads to an apparent nonzero  $2k$  ( $\approx 2 \times 10^{-4}$ ) at the INC phase. However, the assumption of a zero OA all over the range seems to work rather well in both phases, except for a few points near the singularity. We conclude, therefore, that the OA at the INC phase is limited to  $|2k| < 2 \times 10^{-4}$ , which is smaller than the resolution of the measurement. In other words,  $g_{33} = 0$  in the whole temperature range within the experimental error.

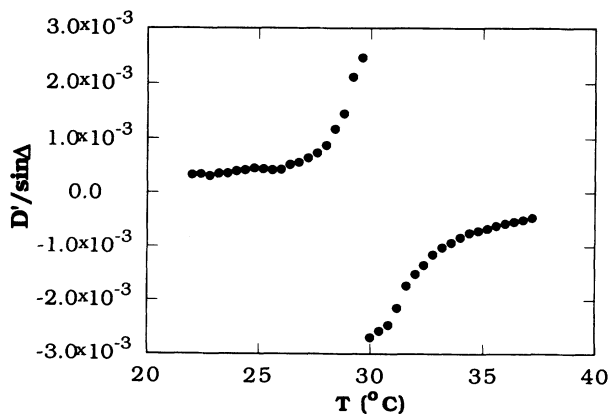


FIG. 9. Temperature dependence of the quantity  $D'/\sin\Delta = -(2k - \gamma) + \delta Y \cot\Delta / 2$  for  $\text{TMAcCl}$ . The singularity at  $30^\circ\text{C}$  is due to the passage of  $\Delta$  through an integer number of  $2\pi$  at this temperature.

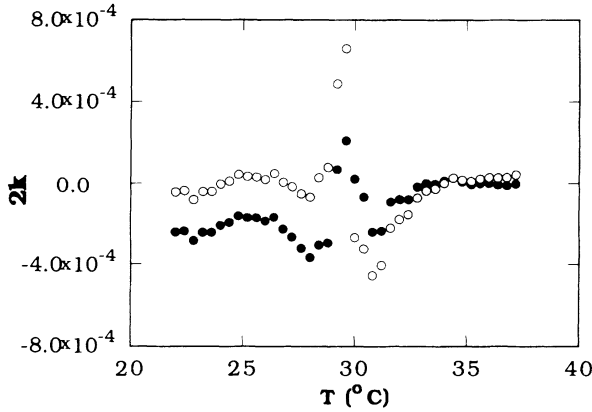


FIG. 10.  $2k$  data of TMAcCuCl viewed along the  $c$  axis. These values were deduced from  $D'/\sin\Delta$  and the error constants  $\gamma$  and  $\delta Y$  obtained by assuming a zero value of the OA in the parent phase (solid symbols) or in the whole temperature range (open symbols).

#### IV. DISCUSSION

The OA results presented here are in marked contrast to those found in the literature for some centrosymmetric INC structures.<sup>2-10</sup> In particular, a nonzero  $g_{13}$  coefficient has been obtained for  $\text{Rb}_2\text{ZnBr}_4$  (Ref. 8), and although no measurements for the  $g_{33}$  coefficient have been reported up to now for TMAcCuCl, OA along the INC wave vector has been observed in the analogous compound with Zn.<sup>10</sup>

In view of these large discrepancies, it seems of interest to examine with attention some aspects of the experimental procedure and measuring process. Although the working principles of our HAUP polarimeter and that described in Refs. 5 and 8 are essentially the same, some differences can be found in the method followed for the data collection and in the procedure used to perform the refinement. Since the size of the effect to be measured is quite small, these differences can lead to important discrepancies in the final results. In our opinion the following points must be treated with special care because they could potentially be sources of systematic errors.

(i) As has been mentioned in Sec. II, no optical components must be placed between the sample and polarizers and even the windows of the cryostat must be suppressed. A simple calculation shows that in the set window sample window between crossed polarizers, the minimum transmitted intensity is achieved for an angle  $\alpha$  between the polarizer and slow axis of the sample given by

$$\alpha = (\delta/4 \sin 2\phi + \delta'/4 \sin 2\phi') \cot \Delta / 2, \quad (5)$$

where  $\delta$  and  $\delta'$  are the optical retardation of the windows,  $\Delta$  the retardation of the sample, and  $\phi$  and  $\phi'$  the angles between the slow axes of the windows and sample. This is equivalent to considering that the windows disturb the quality of the polarizers and induce in them parasitic ellipticities of values  $p = \delta/2 \sin 2\phi$  and  $q = \delta'/2 \sin 2\phi'$ . In order to check this effect, we have

measured the quantity  $(p+q)^2$  for a set of six fused-silica windows of a continuous-flow cryostat. This was obtained by measuring the extinction ratio of the polarizers, which is equal to  $1/4(p+q)^2$ . Figure 11 shows the dependence of  $(p+q)^2$  as a function of the polarizer angle. As can be seen, the results fit fairly well to a function  $a \sin^2(2\phi+b)$ , with  $a$  and  $b$  constants. The value obtained for the  $a$  constant implies a birefringence of the windows of the order of  $10^{-7}$ . Even this small birefringence value, if not taken into account, can completely spoil the measurement. An additional problem is that  $a$  and mainly  $b$  vary with temperature and are also dependent on thermal history. This prevents absolutely any attempt for calibration.

(ii) Light intensities should be measured around the absolute minimum of the  $(\Theta, Y)$  region. This is important because, under the same conditions for errors in the raw data, the absolute error and standard deviation in  $2k$  grow quickly for increasing distance from the centered  $(\Theta, Y)$  grid position.<sup>13</sup>

(iii) The parameters  $C'$  and  $D'/\sin\Delta$  can be obtained without the necessity of starting values (as is the case in Ref. 8) because the refinement can be performed by using a linear least-squares method. We have found that the quality of these fits is usually excellent. On the other hand, by using the kind of adjustment employed by Kobayashi *et al.*, no proper account is taken of correlations between the different coefficients and the values of some parameters (e.g.,  $\Theta_0$ ) depend only on the result performed along a single line of the  $(\Theta, Y)$  surface.<sup>14</sup>

(iv) The  $\delta Y$  error contribution can be important, and the final OA values are specially sensitive to the method used for its removal. In Ref. 8 this error was calculated by averaging all values of  $D' \tan \Delta / 2$  with  $\sin^2 \Delta / 2 < 0.5$ . This is not conventional, and some problems may arise especially if the points scatter a lot. The method suggested by Kobayashi, Kumoni, and Saito<sup>5</sup> is more straightforward and provides a way to check the consistency of the results since  $D'/\sin\Delta$  must be linearly correlated with  $\cot \Delta / 2$ .

As has been mentioned before, non zero  $g_{13}$  values have been reported for centrosymmetric INC compounds.<sup>2-10</sup> The order of magnitude of the correspond-

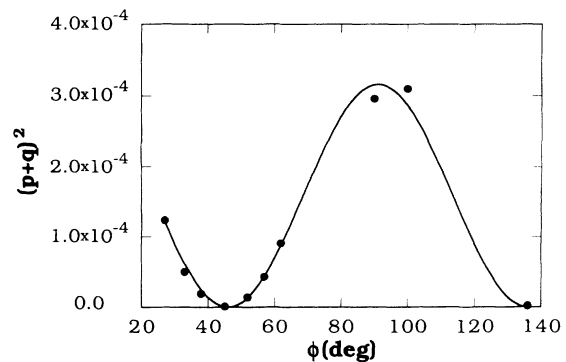


FIG. 11. Polarizer angle dependence of the square of the parasitic ellipticities  $(p+q)^2$  introduced by a set of fused-silica windows of a continuous-flow cryostat. The solid line is the best fit to a function  $a \sin^2(2\phi+b)$ , with  $a$  and  $b$  constants.

ing  $2k$  is typically  $10^{-3}$ . However, it is interesting to point out that there are important discrepancies in the  $g_{13}$  results found in the first<sup>2,4</sup> and later<sup>5,6</sup> works carried out by Kobayashi and co-workers in INC compounds of the  $A_2BX_4$  family. In all cases the OA behavior also differs from the results obtained by other authors.<sup>9</sup>

In the particular case of  $Rb_2ZnBr_4$ , it is evident that our results are in great contrast to those of Ref. 8. The  $2k$  values differ by about two orders of magnitude, and the experimental accuracy is, in our measurements, almost two orders of magnitude higher. It is difficult to explain such a large disagreement as due only to "some problems with the mechanical interface between the stepping motors and the Nicols" mentioned by the authors themselves. In our view the principal cause of the discrepancy is the different consideration of some sources of systematic errors [especially points (ii)-(iv)] in the experimental procedure used in both cases.

The behavior of the  $g_{33}$  coefficient is a question also subject to some controversy. Dijkstra<sup>10</sup> has detected OA along this direction in  $TMAZnCl$ , with  $2k$  as high as  $10^{-2}$  at the middle of the INC phase. Likewise, Hardy, Katkanant, and Edwardson,<sup>23</sup> on the basis of molecular-dynamics studies, have predicted the appearance of gyration effects along the INC modulation direction in some  $A_2BX_4$  compounds. On the other hand, this is in disagreement with the gyration surfaces proposed by Kobayashi<sup>24</sup> for  $TMAZnCl$  (which implies  $g_{33}=0$ ), although, as far as we know, no specific measurement of  $g_{33}$  has ever been published by this group. As has been shown in Sec. III, we have also determined a zero  $g_{33}$  value for  $TMACuCl$ . It is worth noting that the case of  $TMAZnCl$  is rather difficult to deal with experimentally. This is due to the fact that the birefringence of this material passes through zero at the middle of the INC range. Consequently, a singularity of  $\cot\Delta/2$  is inevitable at that point, and therefore, the  $\delta Y$  error contribution is specially important and difficult to remove in that range.

We now turn to the discussion of the different theoretical treatments proposed in the literature to explain the appearance of gyration effects in these materials. We will center the discussion on the approach by Meekes and Janner,<sup>8</sup> which is, by far, the most complete of the theories available and is able to predict, on the basis of symmetry arguments, in which directions nonzero OA must be expected.

The starting point of this theory is the spatial dependence of the gyration and dielectric tensors. The selection rules imposed by the INC superspace group are applied to the long-wavelength Fourier components of these

tensors. In the case of a modulation  $\mathbf{q}=\gamma\mathbf{c}^*$ , the relevant Fourier components correspond to wave vectors  $\mathbf{h}=l\mathbf{c}^*+m\mathbf{q}$ , with  $l, m$  integers. It is supposed that the Fourier contributions are of decreasing importance for increasing  $m$  indices and increasing lengths of the reciprocal lattice vectors  $(0,0,1,m)$ . For  $Rb_2ZnBr_4$ , considering only the first Fourier component ( $l=1, m=-3$ ) a nonzero  $g_{13}(\mathbf{h})$  value is predicted. In the case of  $TMAZnCl$ , with the same superspace group (but with  $\mathbf{q}\approx\frac{2}{3}\mathbf{c}^*$  and then  $l=2, m=-5$ ), all  $g_{ij}(\mathbf{h})$  are allowed.

However, reciprocal lattice vectors such as  $(0,0,1,-3)$  or  $(0,0,2,-5)$  are of quite limited importance in x-ray diffraction, and it is not clear to what extent the Fourier components corresponding to these vectors can have enough size so as to explain the observed magnitude of the gyration, in some cases as large as that of  $\alpha$ -quartz. Furthermore, the corresponding  $2\pi/|\mathbf{h}|$  lengths in real space are as small as 10 nm, which seems to imply the cancellation of these effects in any practical situation.

A variant of this theory has been used by Dijkstra<sup>10</sup> to explain his results for the  $g_{33}$  coefficient in  $TMAZnCl$ . In this work the appearance of a nonzero Fourier component of the dielectric tensor  $\epsilon_{12}(\mathbf{h})$  is exploited. It is shown that this inhomogeneity of the dielectric tensor can give rise to an apparent gyration effect without the necessity of taking into account the  $g_{ij}$  tensor. In this case, thanks to the small value of  $\epsilon_{11}-\epsilon_{22}$  ( $\Delta n\approx 10^{-5}$ ),  $\epsilon_{12}(\mathbf{h})$  does not need to be too large. However, as pointed out by the author himself, the relevant  $2\pi/|\mathbf{h}|$  distance is again very small, and in average, the effects should canceled out to zero.

As a conclusion, we can say that the experimental results in this paper support the view that the symmetry restrictions of gyration tensors in INC structures are those imposed by the point group associated with their superspace symmetry.<sup>25</sup> In order to confirm this point, it would be interesting to examine other INC materials and also to consolidate definitively the experimental procedure to be followed when using the HAUP technique.

#### ACKNOWLEDGMENTS

We thank Dr. J. M. Pérez-Mato for his critical reading of the manuscript. Two of us (J. O. and J. E.) gratefully acknowledge Dr. A. M. Glazer and I. J. Tebbutt for helpful comments about the HAUP method and also for their hospitality during a visit to Clarendon Laboratory. J. O. also thanks the Basque Government for financial support. This work is supported by the Basque Government (Project No. 063.3410-0027-89) and by the Research Funds of Universidad del País Vasco (Project No. 063.310-E030-90).

\*Permanent address: Institute of Physics, A. Mickiewicz University, Grunwaldzka 6, 60-870 Poznan, Poland.

<sup>1</sup>J. Kobayashi and Y. Uesu, *J. Appl. Crystallogr.* **16**, 204 (1983).

<sup>2</sup>Y. Uesu and J. Kobayashi, *Ferroelectrics* **64**, 115 (1985).

<sup>3</sup>J. Kobayashi, Y. Uesu, J. Ogawa, and Y. Nishihara, *Phys. Rev. B* **31**, 4569 (1985).

<sup>4</sup>K. Saito, I. Kunishima, J. Kobayashi, and Y. Uesu, *Ferroelec-*

*trics* **64**, 137 (1985).

<sup>5</sup>J. Kobayashi, H. Kumoni, and K. Saito, *J. Appl. Crystallogr.* **19**, 377 (1986).

<sup>6</sup>J. Kobayashi, K. Saito, H. Fukase, and K. Matsuda, *Phase Transitions* **12**, 225 (1988).

<sup>7</sup>K. Saito, H. Sugiya, and J. Kobayashi, *J. Appl. Phys.* **68**, 732 (1990).

- <sup>8</sup>H. Meekes and A. Janner, *Phys. Rev. B* **38**, 8075 (1988).
- <sup>9</sup>E. Dijkstra and A. Janner, *Ferroelectrics* **105**, 113 (1990).
- <sup>10</sup>E. Dijkstra, *J. Phys. Condens. Matter* **3**, 141 (1991).
- <sup>11</sup>T. Asahi, K. Uchino, J. Kobayashi, and W. Kleemann, *Ferroelectrics* **94**, 329 (1989).
- <sup>12</sup>J. Kroupa, J. Albers, and N. R. Ivanov, *Ferroelectrics* **105**, 345 (1990).
- <sup>13</sup>J. R. L. Moxon, Ph. D. thesis, Oxford University, 1990.
- <sup>14</sup>J. R. L. Moxon and A. R. Renshaw, *J. Phys. Condens. Matter* **2**, 6807 (1990).
- <sup>15</sup>J. R. L. Moxon, A. R. Renshaw, and I. J. Tebbutt, *J. Phys. Condens. Matter* (to be published).
- <sup>16</sup>J. Kobayashi, T. Asahi, S. Takahasi, and A. M. Glazer, *J. Appl. Crystallogr.* **21**, 479 (1988).
- <sup>17</sup>M. Iizumi and K. Gesi, *J. Phys. Soc. Jpn.* **52**, 2526 (1983).
- <sup>18</sup>R. A. Laudise, *The Growth of Single Crystals* (Prentice Hall, Englewood Cliffs, NJ, 1970).
- <sup>19</sup>J. Sugiyama, M. Wada, and Y. Ishibashi, *J. Phys. Soc. Jpn.* **49**, 1405 (1980).
- <sup>20</sup>G. Madariaga (private communication)
- <sup>21</sup>A. Gómez-Cuevas, M. J. Tello, J. Fernández, A. López Echarri, J. Herreros, and M. Couzi, *J. Phys. C.* **16**, 473 (1983).
- <sup>22</sup>O. G. Vlokh, A. V. Kityk, O. M. Mokry, and V. G. Grybyk, *Phys. Status Solidi* **116**, 287 (1989).
- <sup>23</sup>J. R. Hardy, V. Katkanant, and P. J. Edwardson, *Ferroelectrics* **87**, 23 (1988).
- <sup>24</sup>J. Kobayashi, *Phys. Rev. B* **42**, 8332 (1990).
- <sup>25</sup>R. M. Pick, in *Geometry and Thermodynamics: Common Problems in Quasi-Crystals, Liquid Crystals and Incommensurate Systems*, edited by J. C. Toledano (Plenum, New York, 1990), p. 439.